

Femtosecond electron spectroscopy of coronene, benzo[GHI]perylene, and anthracene

M. Kjellberg,¹ A. V. Bulgakov,^{1,2} M. Goto,³ O. Johansson,⁴ and K. Hansen^{1,a)}

¹*Department of Physics, University of Gothenburg, 41296 Gothenburg, Sweden*

²*Institute of Thermophysics SB RAS, Russian Academy of Science, ave. Lavrentyev 1, 630090 Novosibirsk, Russia*

³*Department of Chemistry, Tokyo Metropolitan University, 1-1 Minamiosawa, Hachioji-shi, Tokyo 192-0397, Japan*

⁴*School of Chemistry, University of Edinburgh, Edinburgh EH9 3JJ, United Kingdom*

(Received 24 February 2010; accepted 30 June 2010; published online 20 August 2010)

The large polycyclic aromatic hydrocarbon molecules coronene, benzo[GHI]perylene, and anthracene have been ionized with femtosecond laser pulses at low laser intensities and the ionization process studied with velocity map imaging spectroscopy, supplemented with ion yield measurements. The electron spectra of coronene and benzo[GHI]perylene are structureless. Based on fluence and pulse duration dependence measurements, it is shown that the electron spectra are not produced in field ionization processes, and the ionization mechanism is identified to be a quasithermal statistical electron emission, previously suggested for the fullerenes C_{60} and C_{70} . The anthracene photoelectron spectra are dominated by above threshold ionization features, but with some indication of quasithermal ionization at longer pulses. © 2010 American Institute of Physics. [doi:10.1063/1.3466925]

I. INTRODUCTION

Multiphoton ionization of molecules in short laser pulses is usually assigned to either above threshold ionization (ATI) at low laser intensities¹⁻³ or field ionization at high intensities.⁴⁻⁶ The experimental signature of ATI in photoelectron spectra is a clearly identifiable series of peaks, separated by one photon energy. Field ionization occurs for atoms when the electric field is high enough to cause one or more electrons to move out of the Coulomb potential of the nucleus, in classical over-the-barrier trajectories or by tunneling through a barrier.⁷ The latter process gives rise to a host of interesting phenomena, such as recollisional ionization, and has also been predicted to give rise to spectra with strong, photon energy separated peaks, similar to those observed in the pure ATI phenomenon.⁷

In this work, we present evidence that a third ionization mechanism is important for large organic molecules. It is a thermal emission process that occurs between the time of excitation of electronic states and the coupling of the electronic excitations to vibrational motion. The quantities relevant to describe this ionization mechanism are the electron-electron and the electron-vibration coupling time and the thermal properties of the excited electronic states. Photoelectron spectra of the previously studied fullerenes C_{60} and C_{70} are consistent with this quasithermal emission process,⁸⁻¹⁰ which has also been corroborated in Penning ionization ion yield studies on C_{60} for which the mechanism was originally proposed.¹¹ Photoelectron spectra of sodium clusters¹² and ionization dynamics of rare gas clusters¹³ have similarly been interpreted with this picture.

Although demonstrated to be applicable for fullerenes, the degree of universality of the mechanism is unknown and it is also not known if it is restricted to deep subthreshold ionization processes, i.e., multiphoton ionization processes with photon energies far below the ionization energy (IE). So far, neither has it been known if this type of ionization occurs for molecules composed of more than one element nor at what size the mechanism fails. The main motivation for the work presented here is to investigate these two questions.

The three polycyclic aromatic hydrocarbon (PAH) molecules studied, coronene, benzo[GHI]perylene, and anthracene are all planar. Coronene, $C_{24}H_{12}$, has seven aromatic rings of which six are arranged symmetrically around the central one. Benzo[GHI]perylene, $C_{22}H_{12}$, is similar but with one aromatic ring less, and anthracene, $C_{14}H_{10}$, is a chain of three aromatic rings. The numbers of valence electrons are 108, 100, and 66 for coronene, benzo[GHI]perylene, and anthracene. These molecules were chosen because of their similarity to the fullerenes, the main differences being the size and the added hydrogen.

II. EXPERIMENTAL PROCEDURE

The experiments were performed with a titanium sapphire laser with a minimum pulse duration of 150 fs for the fundamental, a repetition rate of 1 kHz, and a maximum pulse energy of close to 1 mJ. The photon energy of the fundamental infrared beam is 1.6 eV. Both the photoelectron spectra and the ion spectra are recorded with typically 10^5 laser pulses. Usually less than 10% of the maximal laser pulse energy is transmitted through a variable attenuator. Higher transmission leads to substantial fragmentation which precludes a safe identification of the molecular source of the photoelectron. Laser fluences were calibrated once by com-

^{a)}Electronic mail: klavs@physics.gu.se.

parison with literature Xe ion yield data that display a characteristic shape when plotted vs. the laser intensity on a double logarithmic scale. Fluences were in fairly good agreement with values expected from calculations of Gaussian beam propagation and beam characteristics measured outside the vacuum chamber. The laser compression stage could be detuned to provide pulse durations of several picoseconds. The temporal profile was measured with an autocorrelator and the shape found to be well preserved, although not perfectly, also for long pulses.

The electron spectrometer is of the velocity mapping imaging type, similar to the one described by Bordas *et al.*¹⁴ It projects the electron distribution on a two-dimensional position sensitive detector comprised of a pair of microchannel plates and a phosphor screen,¹⁵ in our device, located ca. 20 cm downstream. The electrons are extracted with ca. 2 kV acceleration energy, multiplied by a dual channel plate detector and the spectrum recorded with a charge coupled device (CCD) camera. The laser polarization is parallel with the detector plane, and the cylindrical symmetry allows one to invert the measured two dimensional spectrum to obtain the three dimensional spectrum of the electron momenta emitted by the molecule.¹⁶

A time of flight mass spectrometer is placed back-to-back with the electron spectrometer. The molecular beam, the laser beam and the spectrometers are placed in perpendicular configuration. Ions are detected after a quick switch of the polarity of the electrodes, and the mass spectrometer acceleration is achieved in a three-electrode configuration. The mass spectrometer can be operated in both linear and reflectron mode. The mass resolution is about $m/\delta m \approx 300$, which allows to distinguish loss of hydrogen from a coronene molecule. The spectrometers are described in Ref. 10 which should be consulted for further details.

Mass spectra of all the molecules were recorded at varying fluences, typically between 0.4 and 2 J/cm², but for some up to 10 J/cm². The high fluences serve to determine the pulse durations and fluences where the multiply charged molecules appear in the spectra.

III. CORONENE

Electron spectra of coronene ionized with 775 nm 150 fs light are shown in Fig. 1, both raw data and the corresponding deconvoluted spectra. The derived energy distributions are shown in Fig. 2. The spectra are dominated by a smooth distribution of exponential form for electron kinetic energies greater than the photon energy for the laser intensities below 1×10^{13} W/cm². For the spectra with fluences below that, the Keldysh parameter ranges from 2.8 to 4.1, which is far from the field ionization regime and which is one indication that this phenomenon cannot explain the smooth behavior of the curves. This is very similar to the behavior of the fullerenes under similar conditions.

Thus, the spectra recorded with laser intensities in the multiphoton ionization regime and for single ionization conditions of the coronene molecule, resulted in Boltzmann-like electron distributions with no major contribution from ATI peaks. The observation suggests that the transient hot elec-

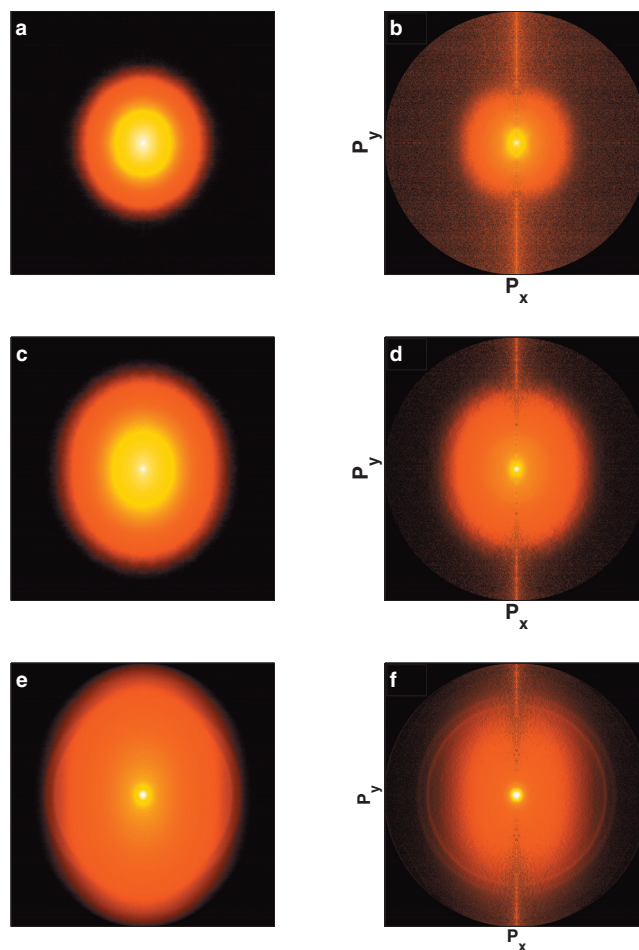


FIG. 1. Electron momentum maps of coronene after 150 fs, 775 nm ionization. Left columns are symmetrized images and right columns are the inverted images. Laser peak intensities are as follows: 0.36 [(a) and (b)], 1.15 [(c) and (d)], and 6.1×10^{13} W/cm² [(e) and (f)].

tron ionization is present also for coronene. The (apparent) electron temperatures extracted from linear fits to the photoelectron distributions are shown in Fig. 3.

For fluences above 1×10^{13} W/cm² two strong pairs of

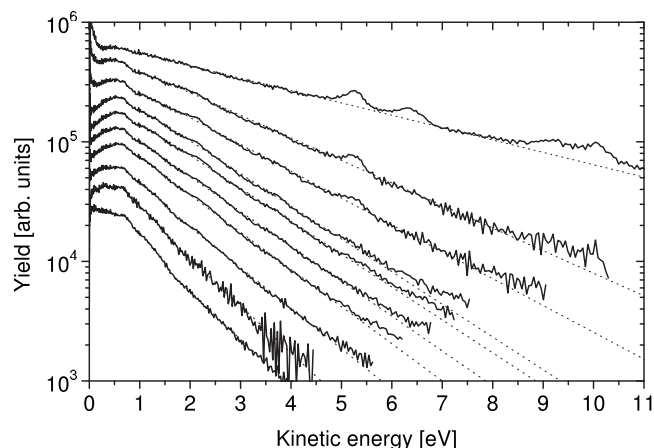


FIG. 2. Electron spectra of coronene at constant pulse duration of 150 fs. Wavelength of 775 nm. From bottom to top the laser intensities are as follows: 3.6, 4.9, 6.7, 8.0, 9.3, 10.9, 12, 21, 28, and 61×10^{12} W/cm². The spectra are shifted vertically for display purposes here and in all other photoelectron spectra.

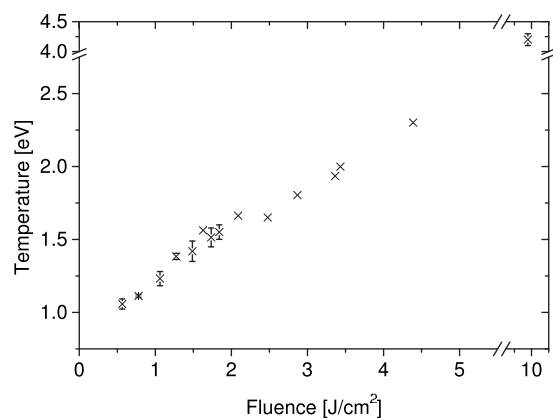


FIG. 3. Electron temperatures of coronene extracted from the spectra in Fig. 2. Error bars refer to reproducibility of the measurements here and in other figures. The relation between fluences and intensities is the pulse duration which in this case is 150 fs, as a multiplicative factor.

peaks appear in the spectra at 5.3/6.3 and 9.3/10.3 eV, superimposed on the smooth distribution. These peaks, which appear when extensive fragmentation is present, are clearly seen as rings in Fig. 1(f) and are commonly present at high fluences for all molecules. Due to their energy and the 1 eV/4 eV separation they cannot originate from ATI with 1.6 eV photons. They show no angular dependence in count rate relative to the laser field polarization and they become pronounced in the electron spectra when C^+ and C^{2+} appear in the mass spectra. The explanation for these peaks is suggested to be an electron recombination process followed by electron emission. The first excited state of C^+ ($^4P\ 2s2p^2$) is at 5.33 eV and the second excited state ($^2D\ 2s2p^2$) at 9.29 eV. The 6.3 eV peak fits rather well with the first excited state of C^{2+} ($^3P^o\ 1s^22s2p$) at 6.50 eV.

In addition to these peaks of atomic origin, the ATI series can be seen as very weak peaks in the fourth spectrum from the top with the first, second, and third peak at energies 2.2, 3.7, and 5.3 eV respectively.

In order to verify the origin of the electrons, mass spectra were measured for several fluences. Mass spectrometry of PAH molecules after femtosecond-laser excitation has been extensively studied before^{17–21} and the results presented here mainly serve as a reference to the photoelectron spectra and for comparison with the fullerene mass spectra.

Mass spectra of coronene after irradiation with 775 nm, 150 fs pulses at different laser intensities are shown in Fig. 4. For the lowest intensity, in Fig. 4(d), only the singly charged mother ion (M^+) is observed. At slightly higher intensity, Fig. 4(c), fragmentation sets in and the doubly charged mother ion M^{2+} appears, together with the doubly charged mother ion with two hydrogen atoms eliminated. At even higher intensities, Figs. 4(a) and 4(b), the doubly charged ion starts to fragment as well and for the highest applied laser fields (not shown in Fig. 4), singly charged carbon and hydrogen atoms and small molecular ions dominate the spectra.

It appears as if there is, as for fullerenes, a competition between fragmentation and a second ionization step of the singly charged mother ion. Once the mother ion reaches the doubly charged state it is unlikely that it will ionize again, due to the high ionization energy of this charge state, or at

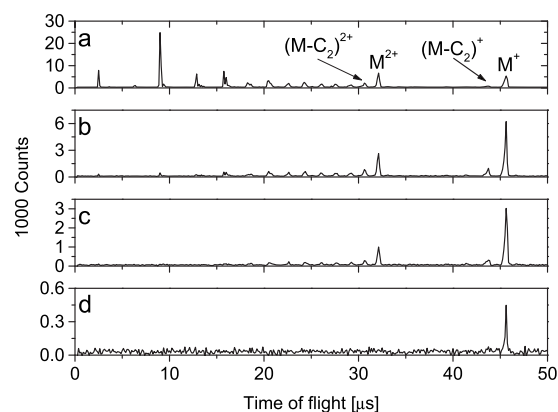


FIG. 4. Mass spectra of coronene after 775 nm and 150 fs laser ionization. Laser intensities are as follows: (a) 2.8×10^{13} , (b) 1.11×10^{13} , (c) 6.7×10^{12} , and (d) 3.3×10^{12} W/cm².

least that the triply ionized species will survive until detection. Hence, the highly excited M^{2+} ion relaxes through fragmentation and a strong signal at smaller masses is observed, as for the fullerenes.

The mass spectra suggest that fluences up to 1×10^{13} W/cm² should be dominated by the singly ionized unfragmented parent molecule. It should be kept in mind when evaluating the mass spectra that the detection efficiency is higher for smaller molecules and higher charges, and that postionization, preacceleration fragmentation must be expected to be present also. The above fluence limit, valid for 150 fs laser pulses is therefore a conservative estimate.

It is possible to make an estimate of the energy residing in the electronic system at the time of electron emission using simple and rather idealized thermal properties of the molecules. We treat the molecule as a Fermi gas with the Fermi energy $E_f = 20$ eV and typical temperatures of 1.5 eV. The measured temperature is that of the ion. The valence electron energy content of the product cation is then

$$E \approx \frac{\pi^2 N_e}{4 E_f} T^2 = 0.28 \text{ eV } N_e, \quad (1)$$

where N_e is the number of valence electrons. The Fermi energy is chosen as a reduced value of the 30 eV of Ref. 11 because of the presence of hydrogen. With $N_e = 108$, 100, and 66 for the three molecules, this gives 19, 17, and 11 photons. Furthermore the energy deposited in the vibrational motion before ionization and the energy absorbed after ionization must be added if one is concerned with postionization fragmentation. The last two are very difficult to determine, even within a simplified theoretical model. A comparison between the electron temperatures and the fragmentation pattern therefore comes with a significant uncertainty but if we for example use the minimal value of 19 photons in the coronene cation $C_{24}H_{12}^+$, the postionization energy per vibrational degree of freedom is about $19 \times 1.6 \text{ eV} / (3(24+12) - 6) = 0.3 \text{ eV}$. This is comparable to the measured values for fullerenes that undergo thermionic emission and fragmentation on the ns time scale.^{22,23} It is therefore plausible that the singly ionized species will show some amount of postionization fragmentation. The small amount of singly charged frag-

ment ions suggest that the unknown amount of energy absorbed is relatively small.

We can also estimate the energy needed to ionize twice and cause the subsequent fragmentation of the doubly charged species. First, we calculate the threshold energy for the second fragmentation of the singly charged molecule in order to see the value of the electronic emission rate constant. Using the energy content of 19 photons in the singly charged molecule, we calculate an energy content for the neutral precursor that would (hypothetically) ionize once and fragment twice to be $19 \times 1.6 + 7.2 + 7 \text{ eV} = 44.6 \text{ eV}$, where the 7.2 eV is used for the ionization energy of coronene²⁴ and the 7 eV is an estimated dissociation energy. The second electron emission will have $44.6 - 7.2 = 37.4 \text{ eV}$ available and with the second ionization energy 11.3 eV,²⁴ this gives a second electron emission rate constant of $8.8 \times 10^{15} \text{ s}^{-1} \exp(-11.3 \text{ eV}/1.53 \text{ eV}) = 5.4 \times 10^{12} \text{ s}^{-1} = 1/180 \text{ fs}$, where the frequency factor is twice that of the singly charged molecule because of the correspondingly larger electron capture cross section,⁹ and the emission temperature is the average of the singly and doubly charged molecule. This is indeed on the order of the expected coupling time and indicates that if the molecule's electronic system absorbs enough energy for the molecule to fragment twice, it will instead ionize twice with a high probability.

We can estimate the amount of energy required to ionize twice by calculating the temperature needed to give a rate constant of 10^{13} s^{-1} . The value is 2.4 eV and the corresponding energy is 74 eV for the doubly charged ion. This is enough to cause a larger number of fragmentation processes, consistent with the tail of fragments seen for the doubly charged.

We conclude from these, admittedly crude estimates, that the fragmentation pattern and charge pattern is consistent with the proposed ionization mechanism.

The values of the Keldysh parameter in our experiments suggest that field ionization is not the dominant mechanism below the fluences where the ATI peaks are observed. It is nevertheless highly desirable to have more direct evidence for the nature of the mechanisms by which the electrons are emitted, also because of the theoretical uncertainty surrounding the relevance of the Keldysh parameter in connection with ionization of molecules as opposed to ionization of atoms. We will use a signature based on the different behavior of the two ionization mechanisms when the pulse duration is changed. Field ionization probes the instantaneous value of the electric field, at least compared to time scales of tens or hundreds of femtoseconds, whereas a quasithermal ionization probes the amount of energy which is absorbed and not yet dissipated into vibrational motion. Thus, if field ionization is responsible for the measured spectra, we see a stretched laser pulse is expected to produce the same electron spectra as a short laser pulse with the same intensity. Obviously, the electron yields will be different but not the shape of the electron spectra. Conversely, if the electron spectra are emitted in a quasi-thermal process, the longer pulse will produce a higher apparent temperature than the shorter pulse, by virtue of the larger energy content.

Electron spectra were therefore measured for different

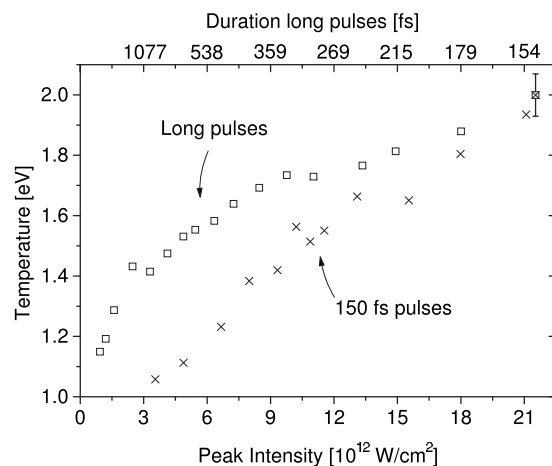


FIG. 5. The measured coronene electron temperatures vs laser peak intensity. Crosses: varying fluence at 150 fs pulse duration. Open squares: varying pulse duration at the fixed laser fluence 3.4 J/cm^2 .

pulse durations between 150 fs and 3.5 ps, and the apparent temperatures in the spectra fitted. As for short pulses, the long pulse electron energy distributions, the part above the photon energy, are clearly dominated by a thermal distribution. Note that the use of a temperature does not bias the test; it is simply used as a convenient shorthand for the shape of the spectra. The results of such an experiment on coronene are shown in Fig. 5. For identical peak intensities, the laser pulse with the longest pulse duration (highest fluence) generates the highest electron temperature. For the lowest temperatures observed, around 1.2–1.3 eV, the short 150 fs pulse needs to be 4 times more intense than the more energetic stretched pulses to give the same electron temperature. The highest intensities used in this study mean that rigorously speaking one could disregard the high temperature data because the extended fragmentation throws some doubt on the nature of the molecule from which the electron originates. The separation of the two branches at low temperatures is, however, unaffected by this effect and guarantees the rigor of the test. The evidence therefore clearly points to a quasithermal process.

IV. BENZO[GHI]PERYLENE

The measurements of photoelectron spectra of benzo[GHI]perylene with the laser fundamental wavelength mirror those performed on coronene. In addition, measurements were performed with the doubled frequency, 3.2 eV, 388 nm. The benzo[GHI]perylene has a molecular structure which is similar to coronene's and no major differences were expected between the two molecules in these studies. This expectation was borne out. Photoelectron spectra (PES) are generally structureless above the one photon energy, both for the fundamental and the frequency doubled light, and for short and long pulses alike. One minor, but still clear, difference is that the ATI peaks are slightly enhanced compared to the coronene PES, although they are still very weak.

The test of electron temperatures vs. the peak intensity was also performed for benzo[GHI]perylene. The result, shown in Fig. 6, is similar to the results for coronene, i.e., the smooth parts of the spectra are not due to field ionization.

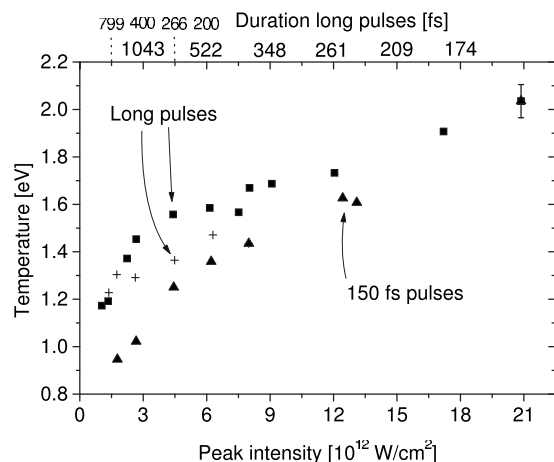


FIG. 6. The electron temperatures from the stretched pulse spectra and from the fixed pulse duration temperatures vs fluence data, both for the fundamental wavelength and plotted vs the intensity. Triangles: varying fluence at 150 fs pulse duration. Crosses: varying pulse duration at fixed laser fluence, 1.3 J/cm². Squares: varying pulse duration at the fixed laser fluence, 3.3 J/cm². The crosses are data for smaller laser fluence than those of the squares. The small font pulse duration on top refer to the crosses and the large font values to the 1.3 J/cm² data.

The momentum maps of benzo[GHI]perylene for four different laser intensities of the second harmonic are shown in Fig. 7. Corresponding photoelectron spectra are shown in Fig. 8. For all laser intensities the asymmetry in the momentum maps which is present in spectra recorded with the fundamental is strongly reduced. This may be ascribed to the significantly lower laser intensities needed to ionize with the frequency doubled light, about one order of magnitude. The higher photoabsorption cross section for 388 nm is also apparent in Fig. 9 where the temperature vs. fluence is shown for both wavelengths. Apart from the symmetry, the PES are very similar to the ones obtained with the 775 nm light. For the spectrum corresponding to the highest laser intensity 3.7×10^{13} W/cm², the two non-ATI peaks at 5.3/6.3 eV appear again.

The mass spectra for 775 nm, 150 fs ionization of benzo[GHI]perylene are very similar to those of coronene and will therefore not be discussed in detail. The frequency doubled light was also used to record mass spectra. The intensities used for the 388 nm pulses were ca. one order of magnitude lower than those of the fundamental wavelength pulses. At that reduced pulse energy the spectra are very similar to the ones for 775 nm ionization, both in shape and dependence on laser intensity. One difference is that the doubly charged parent ion is more abundant relative to the lighter fragments, compared to what is observed at any intensity in the IR-light spectra. Also, for the highest intensity, 9×10^{12} W/cm², triply charged carbon appears. For the 1.6 eV photon, 150 fs, pulses the fluence for the crossover to extensive fragmentation was found to lie slightly below that of coronene, at about $7-8 \times 10^{12}$ W/cm².

V. ANTHRACENE

The electron spectra of anthracene after 150 fs, 775 nm ionization are shown in Fig. 10. The electron spectra are dominated by series of ATI peaks for the intensities up to ca.

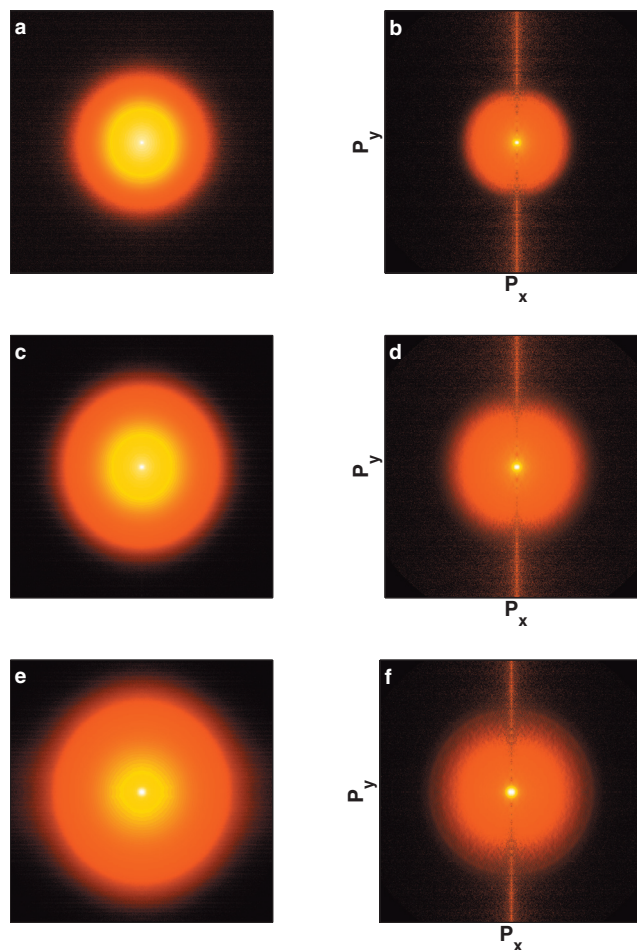


FIG. 7. Electron momentum maps of benzo[GHI]perylene after 150 fs, 388 nm ionization. Left columns are symmetrized images and right columns are the inverted images. Laser peak intensities are as follows: 0.43 [(a) and (b)], 6.6 [(c) and (d)], and 37×10^{12} W/cm² [(e) and (f)].

10^{13} W/cm². Comparing the photoelectron spectra of anthracene in Fig. 10 at relatively low laser intensities to those of the fullerenes C₆₀ and C₇₀ and coronene and benzo[GHI]perylene, it is clear that the transient hot electron emission is not as dominant relative to the ATI process. The fact that the ATI peaks become more dominant for anthracene than for the larger molecules may be related to the reduced density of excited electronic states. The results pre-

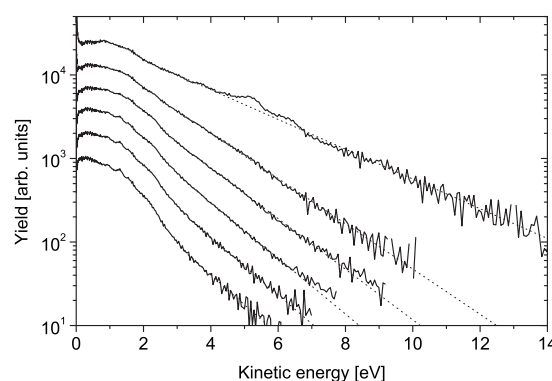


FIG. 8. Electron spectra of benzo[GHI]perylene, 150 fs and 388 nm. From bottom to top the laser intensities are 0.43, 0.76, 1.3, 2.2, 6.6, and 37×10^{12} W/cm².

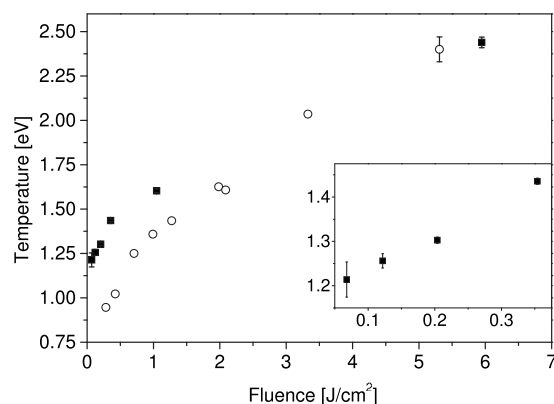


FIG. 9. Apparent electronic temperatures for benzo[GHI]perylene. Solid squares, 388 nm excitation and open circles, 775 nm excitation. The inset shows the 388 nm data for the four lowest fluences. The same intensity calibration was used for the fundamental and the doubled frequencies, except that the latter was multiplied by 4.

sented here are in agreement with the electron spectra reported elsewhere^{25–27} where smaller molecules were observed to give enhanced ATI peak structures.

At higher laser intensities the spectra are smeared out to a smooth distribution of exponential form. It is not possible to say what causes this transition but candidates are tunneling ionization or the onset of a strong thermal ionization process.

ATI and a transient hot electron ionization mechanism can be active at the same time, and the strong ATI peaks in the anthracene spectra do not exclude a thermal component for anthracene. To investigate this, measurements with stretched laser pulses were performed. ATI peaks were present in all measured spectra, but with an amplitude that differed for short and long pulses. This is illustrated in Fig. 11 where spectra of different pulse duration but similar logarithmic slopes were chosen. The pulse durations span from 150 fs to 1.5 ps. In spite of the poor statistics at the long pulses, the contrast between the background and the ATI peak amplitude clearly correlates with the pulse duration. We tentatively take this as evidence for a suppression of the ATI mechanism at long pulses relative to quasithermal ionization.

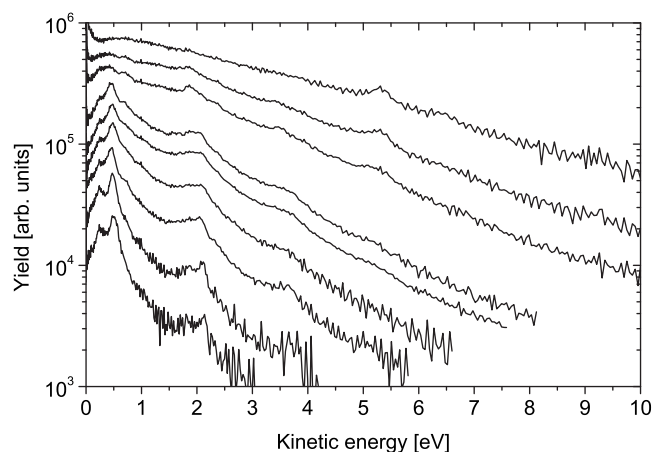


FIG. 10. Electron spectra of anthracene at constant pulse duration of 150 fs. Wavelength of 775 nm. From bottom to top the laser intensities are as follows: 1.8, 3.1, 4.4, 8.0, 9.3, 11, 21, 27, and 61×10^{12} W/cm².

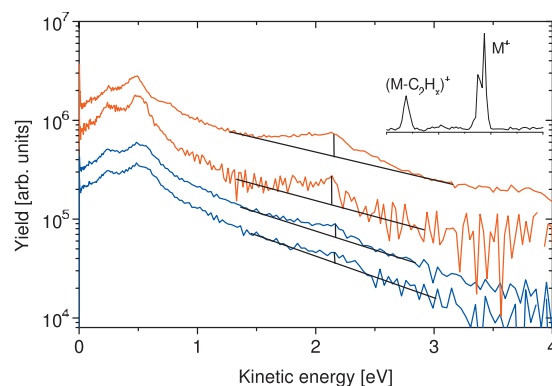


FIG. 11. Electron spectra of anthracene for long laser pulses (blue lines) together with two 150 fs reference spectra (red lines). From top to bottom, the laser pulse durations and intensities are in units of (femtosecond, 10^{12} W/cm²): (150, 4.4), (150, 1.8), (1100, 0.78), and (1490, 0.58). Vertical lines indicate the height of the second ATI-peak which is seen to depend on pulse duration. Inset: mass spectrum corresponding to ionization with a 1.49 ps/ 3.8×10^{11} W/cm² pulse, demonstrating the absence of potentially contaminating thermionic emission electrons.

The mass spectra of anthracene are similar to those reported in the literature for similar laser parameters¹⁹ and will not be shown. The differences to coronene and benzo[GHI]perylene are first of all that anthracene ionizes at lower laser intensity. This is not caused by a lower ionization energy because the IE of anthracene, 7.44 eV,²⁸ is similar to both coronene, 7.39 eV (Ref. 29) or 7.2 eV,²⁴ and benzo[GHI]perylene, 7.2.³⁰ It is however consistent with the results presented in Refs. 31–33, where it was reported that it is easier to ionize smaller molecules with fewer delocalized electrons. The explanation given by the authors is that this is an effect of the reduced screening due to a lower electron number. The onset of extensive fragmentation, however, seems to have shifted much less and is similar to the two larger molecules.

VI. CONCLUSION

The large molecules coronene and benzo[GHI]perylene ionize with smooth electron spectra after fs laser excitation, similarly to C₆₀ and C₇₀. These smooth spectra were shown not to be due to field ionization but are consistent with the transient hot electron ionization mechanism previously observed for fullerenes. For the smaller molecule anthracene, the ATI series become significantly more dominant in the electron spectra, although a smooth component is present for long laser pulses.

ACKNOWLEDGMENTS

This work has been supported by the Swedish Research Council (VR), the Gothenburg Nanoparticle Platform, Stiftelsen för Internationalisering av högre utbildning och forskning (STINT), the Royal Swedish Academy (KVA), and EastChem. We thank E. E. B. Campbell for the assignment of the non-ATI peaks.

¹P. Agostini, F. Fabre, G. Mainfray, G. Petite, and N. K. Rahman, *Phys. Rev. Lett.* **42**, 1127 (1979).

²W. Becker, F. Grasbon, R. Kopold, D. B. Milosevic, G. G. Paulus, and H. Walther, *Adv. At., Mol., Opt. Phys.* **48**, 35 (2002).

- ³R. R. Freeman, P. H. Bucksbaum, H. Milchberg, S. Darack, D. Schumacher, and M. E. Geusic, *Phys. Rev. Lett.* **59**, 1092 (1987).
- ⁴L. V. Keldysh, *Sov. Phys. JETP* **20**, 1307 (1965).
- ⁵P. B. Corkum, *Phys. Rev. Lett.* **71**, 1994 (1993).
- ⁶C. I. Blaga, F. Catoire, P. Colosimo, G. G. Paulus, H. G. Muller, P. Agostini, and L. F. DiMauro, *Nat. Phys.* **5**, 335 (2009).
- ⁷F. H. M. Faisal and G. Schlegel, *J. Mod. Opt.* **53**, 207 (2006).
- ⁸E. E. B. Campbell, K. Hansen, K. Hoffmann, G. Korn, M. Tchapyguine, M. Wittmann, and I. V. Hertel, *Phys. Rev. Lett.* **84**, 2128 (2000).
- ⁹K. Hansen, K. Hoffmann, and E. E. B. Campbell, *J. Chem. Phys.* **119**, 2513 (2003).
- ¹⁰M. Kjellberg, O. Johansson, F. Jonsson, A. V. Bulgakov, C. Bordas, E. E. B. Campbell, and K. Hansen, *Phys. Rev. A* **81**, 023202 (2010).
- ¹¹J. M. Weber, K. Hansen, M.-W. Ruf, and H. Hotop, *Chem. Phys.* **239**, 271 (1998).
- ¹²M. Maier, M. Schätzel, G. Wrigge, M. Astruc Hoffmann, P. Didier, and B. V. Issendorff, *Int. J. Mass. Spectrom.* **252**, 157 (2006).
- ¹³T. Laarmann, M. Rusek, H. Wabnitz, J. Schulz, A. R. B. de Castro, P. Gürtler, W. Laasch, and T. Möller, *Phys. Rev. Lett.* **95**, 063402 (2005).
- ¹⁴B. Bagueard, J. B. Wills, F. Pagliarulo, F. Lépine, B. Climen, M. Barbaire, C. Clavier, M. A. Lebeault, and C. Bordas, *Rev. Sci. Instrum.* **75**, 324 (2004).
- ¹⁵H. Helm, N. Bjerre, M. J. Dyer, D. L. Huestis, and M. Saeed, *Phys. Rev. Lett.* **70**, 3221 (1993).
- ¹⁶C. Bordas, F. Paulig, H. Helm, and D. L. Huestis, *Rev. Sci. Instrum.* **67**, 2257 (1996).
- ¹⁷M. Castillejo, S. Couris, E. Koudoumas, and M. Martín, *Chem. Phys. Lett.* **289**, 303 (1998).
- ¹⁸K. W. D. Ledingham, D. J. Smith, R. P. Singhal, T. McCanny, P. Graham, H. S. Kilic, W. X. Peng, A. J. Langley, P. F. Taday, and C. Kosmidis, *J. Phys. Chem. A* **103**, 2952 (1999).
- ¹⁹M. J. DeWitt and R. J. Levis, *J. Chem. Phys.* **110**, 11368 (1999).
- ²⁰A. N. Markevitch, N. P. Moore, and R. J. Levis, *Chem. Phys.* **267**, 131 (2001).
- ²¹M. Murakami, R. Mizoguchi, Y. Shimada, T. Yatsuhashi, and N. Nakashima, *Chem. Phys. Lett.* **403**, 238 (2005).
- ²²F. Lépine and C. Bordas, *Phys. Rev. A* **69**, 053201 (2004).
- ²³K. Hansen and O. Echt, *Phys. Rev. Lett.* **78**, 2337 (1997).
- ²⁴D. Schröder, J. Loos, H. Schwarz, R. Thissen, D. V. Preda, L. T. Scott, D. Caraiman, M. V. Frach, and D. K. Böhme, *Helv. Chim. Acta* **84**, 1625 (2001).
- ²⁵M. J. DeWitt and R. J. Levis, *Phys. Rev. Lett.* **81**, 5101 (1998).
- ²⁶D. Mathur, T. Hatamoto, M. Okunishi, G. Prümper, T. Lischke, K. Shimada, and K. Ueda, *J. Phys. Chem. A* **111**, 9299 (2007).
- ²⁷T. Hatamoto, M. Okunishi, T. Lischke, G. Prümper, K. Shimada, D. Mathur, and K. Ueda, *Chem. Phys. Lett.* **439**, 296 (2007).
- ²⁸J. W. Hager and S. C. Wallace, *Anal. Chem.* **60**, 5 (1988).
- ²⁹E. Clar, J. M. Robertson, R. Schloegl, and W. Schmidt, *J. Am. Chem. Soc.* **103**, 1320 (1981).
- ³⁰R. Boschi, J. N. Murrell, and W. Schmidt, *Faraday Discuss. Chem. Soc.* **54**, 116 (1972).
- ³¹S. M. Hankin, D. M. Villeneuve, P. B. Corkum, and D. M. Rayner, *Phys. Rev. A* **64**, 013405 (2001).
- ³²S. M. Hankin, D. M. Villeneuve, P. B. Corkum, and D. M. Rayner, *Phys. Rev. Lett.* **84**, 5082 (2000).
- ³³M. Lezius, V. Blanchet, Misha Yu. Ivanov and Albert Stolow, *J. Chem. Phys.* **117**, 1575 (2002).